



ELSEVIER

Contents lists available at ScienceDirect

Physics Letters B

journal homepage: [www.elsevier.com/locate/physletb](http://www.elsevier.com/locate/physletb)

# Emergence of triaxiality in $^{74}\text{Se}$ from electric monopole transition strengths

N. Marchini<sup>a,b,c,\*</sup>, A. Nannini<sup>a</sup>, M. Rocchini<sup>a</sup>, T.R. Rodríguez<sup>d</sup>, M. Ottanelli<sup>a</sup>, N. Gelli<sup>a</sup>, A. Perego<sup>a,b</sup>, G. Benzoni<sup>e</sup>, N. Blasi<sup>e</sup>, G. Bocchi<sup>e</sup>, D. Brugnara<sup>f</sup>, A. Buccola<sup>a,b</sup>, G. Carozzi<sup>f,g</sup>, A. Goasduff<sup>f</sup>, E.T. Gregor<sup>f,1</sup>, P.R. John<sup>g,h</sup>, M. Komorowska<sup>i</sup>, D. Mengoni<sup>g,h</sup>, F. Recchia<sup>g,h</sup>, S. Riccetto<sup>j,k,2</sup>, D. Rosso<sup>f</sup>, A. Saltarelli<sup>c,j</sup>, M. Siciliano<sup>f,g,3</sup>, J.J. Valiente-Dobón<sup>f</sup>, I. Zanon<sup>f,g</sup>

<sup>a</sup> INFN Sezione di Firenze, Firenze, IT-50019, Italy

<sup>b</sup> Università degli Studi di Firenze, Dipartimento di Fisica, Firenze, IT-50121, Italy

<sup>c</sup> Università degli Studi di Camerino, Dipartimento di Fisica, Camerino, IT-62032, Italy

<sup>d</sup> Departamento de Estructura de la Materia Física Térmica y Electrónica and IPARCOS, Universidad Complutense de Madrid, Madrid, E-28040, Spain

<sup>e</sup> INFN Sezione di Milano, Milano, IT-20133, Italy

<sup>f</sup> INFN Laboratori Nazionali di Legnaro, Padova, IT-35020, Italy

<sup>g</sup> Università degli Studi di Padova, Dipartimento di Fisica, Padova, IT-35122, Italy

<sup>h</sup> INFN Sezione di Padova, Padova, IT-35122, Italy

<sup>i</sup> Heavy Ion Laboratory, University of Warsaw, Warszawa, PL-02-093, Poland

<sup>j</sup> INFN Sezione di Perugia, Perugia, IT-06123, Italy

<sup>k</sup> Università degli Studi di Perugia, Dipartimento di Fisica e Geologia, Perugia, IT-06123, Italy

## ARTICLE INFO

### Article history:

Received 14 April 2023

Received in revised form 3 July 2023

Accepted 4 July 2023

Available online 11 July 2023

Editor: B. Blank

### Keywords:

Electric monopole ( $E0$ ) transitions

Internal conversion

Nuclear structure

## ABSTRACT

The structure of  $^{74}\text{Se}$  at low energy was investigated via spectroscopy of internal conversion electrons at the INFN Legnaro National Laboratories (LNL). A set of internal K-conversion coefficients and monopole transition strengths was measured. A large  $\rho^2(E0; 2_2^+ \rightarrow 2_1^+) \cdot 10^3 = 210(130)$  value was deduced. This result, in addition to a low upper limit for the  $0_3^+ \rightarrow 0_2^+$  electron transition, casts in doubt a simple interpretation of the  $^{74}\text{Se}$  low-lying structure, in particular the recently proposed spherical, vibrational character. New microscopic beyond-mean-field calculations generally agree with the experimental results and are capable of producing a large  $\rho^2(E0; 2_2^+ \rightarrow 2_1^+)$  value, even if still a factor  $\approx 7$  smaller than the experiment. Triaxiality and a complex shape-coexistence and mixing scenario seem responsible for this unexpected experimental result.

© 2023 The Author(s). Published by Elsevier B.V. This is an open access article under the CC BY license (<http://creativecommons.org/licenses/by/4.0/>). Funded by SCOAP<sup>3</sup>.

## 1. Introduction

The  $2_2^+$  state in non-doubly-magic, even-even nuclei is commonly interpreted as due to a collective excitation. In the vibrational and rotational limits, this state originates from vibrations around the ground-state shape. Specifically, for a spherical-harmonic vibrator, it is part of the two-phonon multiplet  $J =$

$0^+, 2^+, 4^+$ . Instead, for an axially-symmetric rotor, it is the head of the  $K = 2$  band  $J = 2^+, 3^+, 4^+, 5^+, 6^+, \dots$  – the so-called  $\gamma$  band – resulting from vibrations in the  $\gamma$  degree of freedom. Even though these basic paradigms are known to represent only a first-order approximation of the nuclear structure, they are still used for classifying isotopes throughout the chart of the nuclides and as a basis for more complex theoretical approaches. Nevertheless, since the appearance of low-energy nuclear vibrations has been debated in the recent literature (specifically oscillations around the spherical shape [1–3] and oscillations in the  $\beta$  degree of freedom in axially-symmetric deformed nuclei [4]), the possible vibrational interpretation of the  $2_2^+$  state also needs to be carefully reanalysed.

Monopole transitions ( $E0$ ) are an ideal tool to investigate nuclear structure because they are related to the radial distribution of the electric charge inside the nucleus. Therefore, monopole transition strengths  $\rho^2(E0)$  are sensitive to changes in the shape of the

\* Corresponding author at: INFN Sezione di Firenze, Firenze, IT-50019, Italy.

E-mail address: [marchini@fi.infn.it](mailto:marchini@fi.infn.it) (N. Marchini).

<sup>1</sup> Present address: GSI Helmholtzzentrum für Schwerionenforschung, Darmstadt, 64291, Germany.

<sup>2</sup> Present address: Department of Physics, Queen's University, Kingston, ON K7L 3N6, Canada.

<sup>3</sup> Present address: Argonne National Laboratory, Argonne (IL), 60439, United States.

nuclear states. In particular, this observable is zero if the shape of the two states involved is the same and/or if there is no configuration mixing between their wavefunctions [5]. Noteworthy, the  $\rho^2(E0)$  value between the first two  $2^+$  states is zero in both the vibrational and axially-symmetric rotational limits [6]. A surprising result has been recently obtained in the Ni isotopic chain [7,8], where large  $\rho^2(E0; 2_2^+ \rightarrow 2_1^+)$  values, according to the definition given in Ref. [9], have been measured:  $230_{-80}^{+50} \cdot 10^{-3}$  in  $^{58}\text{Ni}$ ,  $150_{-110}^{+50} \cdot 10^{-3}$  in  $^{60}\text{Ni}$ , and  $140_{-70}^{+50} \cdot 10^{-3}$  in  $^{62}\text{Ni}$ . This outcome is particularly interesting since the investigated isotopes are interpreted as having a spherical shape in their ground states [10–12]. Also, for  $^{58,60}\text{Ni}$  there is no excited  $0^+$  state below the  $2_2^+$  state and, therefore, the shape-coexistence interpretation is excluded. Apart from simple models, a more sophisticated method based on the shell model was also applied to explain these large  $\rho^2(E0)$  values [7], unsuccessfully. This issue is still a puzzle, also due to the lack of systematic data on  $\rho^2(E0)$  values between  $2^+$  states in mid-mass nuclei (see, e.g., Ref. [9]).

Selenium isotopes are thought to be collective in their low-lying structure. Which kind of collectivity, however, is still a matter of debate. A nearly spherical-vibrational scenario was suggested for  $^{74}\text{Se}$  in a recent  $\beta$ -decay study [13]. The anomalous low energy of the  $0_2^+$  state, which is a member of the two-phonon multiplet in this case, was explained as due to the mixing between the  $0_2^+$  state and the intruder, strongly-deformed  $0_3^+$  state. While this interpretation explains several observables in  $^{74}\text{Se}$ , others are not reproduced. If this picture is correct, the  $\rho^2(E0; 2_2^+ \rightarrow 2_1^+)$  value should be negligible and the  $\rho^2(E0; 0_3^+ \rightarrow 0_2^+)$  value should be large. Noteworthy, former studies identified the  $0_2^+$  state as another shape-coexisting state [14,15], and the  $2_2^+$  state as the band-head of a  $\gamma$ -band with on top a sequence of even  $J = 4^+, 6^+$  and odd  $J = 3^+, 5^+, \dots, 15^+$  states [15]. Recent theoretical and experimental investigations indicate the coexistence of prolate and oblate shapes in the proton-rich  $^{68,70,72}\text{Se}$  [16–19] isotopes, while a significant triaxial component has been found in the prolate ground state of  $^{76}\text{Se}$  [20]. Given the most recent suggestions regarding the appearance of multiple-shape coexistence in the neighbouring Ni isotopes [21,22], and the emerging role of triaxiality the close Ge and Zn isotopes [23–26], further investigation in  $^{74}\text{Se}$  is required.

This Letter presents new experimental results regarding internal conversion coefficients and monopole transition strengths in  $^{74}\text{Se}$ . A large  $\rho^2(E0; 2_2^+ \rightarrow 2_1^+)$  value has been measured, with a magnitude comparable to those in the close Ni isotopes [7,8], while the  $\rho^2(E0; 0_3^+ \rightarrow 0_2^+)$  value has been deduced to be small. Also, we performed for the first time microscopic Beyond-Mean-Field (BMF) calculations for  $^{74}\text{Se}$ , and discuss the role of triaxiality in this isotope.

## 2. Experiment

The levels of interest were populated in the  $\beta^+$  decay of  $^{74}\text{Br}$  produced via the  $^{60}\text{Ni}(^{16}\text{O}, pn)^{74}\text{Br}$  reaction. The  $^{16}\text{O}$  beam with 45-MeV energy and 150-enA intensity was provided by the Tandem-XTU accelerator at the INFN Legnaro National Laboratory (LNL). The target was self-supporting with a thickness of 1 mg/cm<sup>2</sup>. The  $^{74}\text{Br}$  ground state has spin and parity  $J^\pi = (0^-)$  and  $T_{1/2} = 25.4$  min [27]. The  $J^\pi = 4^{(+)}$  isomeric state with  $T_{1/2} = 46$  min [27] was populated as well. The experimental setup consisted of a coaxial HPGe detector for  $\gamma$  rays and a magnetic electron spectrometer [28]. In the spectrometer, the internal conversion electrons emitted in the de-excitation of the states enter the magnetic field produced by two electromagnets and are focused onto a 500-mm<sup>2</sup> × 6-mm Si(Li) detector cooled down to the liquid nitrogen temperature. The energy range of the transmitted electrons is varied by changing the current in the electromagnets.

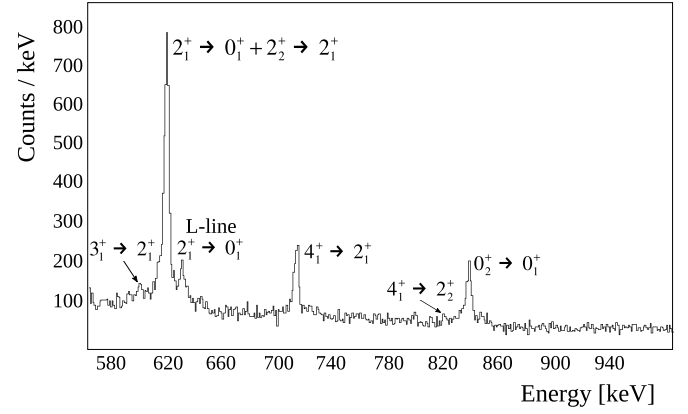


**Fig. 1.** Portion of the electron energy spectrum with the setting of the magnetic field optimised to observe the  $4_1^+ \rightarrow 2_1^+$  transition. K-conversion lines are labelled with spin and parity of the initial and final states. For the  $2_1^+ \rightarrow 0_1^+$  transition, the L-line is visible, too.

**Table 1**

Experimental K-internal conversion coefficients  $\alpha_K$  obtained in the present work for transitions in  $^{74}\text{Se}$  ( $\alpha_K^{\text{exp}}$ ) compared with the calculated values from BRICC [29] for E2, M1 and E1 multipolarities ( $\alpha_K^{\text{th}}$ ). The state at 2563 keV is indicated as ( $2^+, 3, 4^+$ ) as reported in Ref. [27].

$J_i^\pi \rightarrow J_f^\pi$	$E_\gamma$ [keV]	$\alpha_K^{\text{exp}} \cdot 10^3$	$\alpha_K^{\text{th}} \cdot 10^3$		
			E2	M1	E1
$3_1^+ \rightarrow 2_2^+$	615	1.4(4)	1.32(2)	0.97(1)	
$2_2^+ \rightarrow 2_1^+$	634	1.6(2)	1.21(2)	0.90(1)	
$4_1^+ \rightarrow 2_1^+$	728	0.84(7)	0.83(1)		
$4_1^+ \rightarrow 4_2^+$	745	0.99(43)	0.78(1)	0.634(9)	
$4_1^+ \rightarrow 2_2^+$	839	0.55(16)	0.575(8)		
$2_2^+ \rightarrow 0_2^+$	985	0.39(9)	0.388(6)		
$(2^+, 3, 4^+) \rightarrow 4_1^+$	1200	0.26(8)	0.248(4)	0.234(4)	0.116(2)
$3_1^+ \rightarrow 2_1^+$	1250	0.22(6)	0.227(4)	0.216(3)	
$2_2^+ \rightarrow 0_1^+$	1269	0.22(6)	0.220(3)	0.209(3)	
$(2^+, 3, 4^+) \rightarrow 2_1^+$	1294	0.27(12)	0.211(3)	0.201(3)	0.101(2)

Electrons of energy up to  $\sim 2$  MeV are transmitted with an overall 1% efficiency almost constant in the 150–1500 keV range. The system has a momentum acceptance of  $\Delta p/p = 0.18$ , and the Si(Li) detector had a FWHM of 2.6 keV at 1450-keV energy. The HPGe detector was used to detect  $\gamma$  rays de-exciting the states of interest to measure K-conversion coefficients  $\alpha_K$ . This detector had a resolution of 2.2 keV at 1332-keV energy, and it was placed 1 meter away from the target. The measurement was performed by alternating a 60-min irradiation period and a 60-min period with the beam off to observe the decay. The full cycle was repeated using an automated procedure. Electron energy spectra were recorded for different magnetic field settings over a suitable range to cover the electron energies of interest. The spectrum with the optimal settings to observe the  $4_1^+ \rightarrow 2_1^+$  transition is shown in Fig. 1.

## 3. Results

The experimental  $\alpha_K$  values measured in this work are summarized in Table 1 and compared with the calculated values from the Band-Raman Internal Conversion Coefficients (BRICC) database [29] for E1, M1, and E2 multipolarities. The  $\alpha_K$  values have been evaluated using the Normalized-Peak-to-Gamma (NPG) method [30]. The  $\gamma$ -ray and electron intensities have been normalized to the  $13/2^+ \rightarrow 5/2^-$  transition (1064 keV) of a  $^{207}\text{Bi}$  source used for calibration. In the NPG expression, only efficiency ratios appear. Therefore, absolute efficiencies can be replaced by relative ones.

The extraction of the  $\alpha_K(2_2^+ \rightarrow 2_1^+)$  value reported in Table 1 was particularly challenging because the energies of the  $2_2^+ \rightarrow 2_1^+$  and  $2_1^+ \rightarrow 0_1^+$  transitions are practically the same (634.31 keV and

**Table 2**

The  $q^2(E0/E2)$  values and monopole strengths  $\rho^2(E0)$  extracted in the present work are compared with those reported in the literature (Ref. [9]). The  $J_i \rightarrow 2_1^+$  electron transition has been used as the reference  $E2$  transition to the denominator of  $q^2(E0/E2)$ .

$J_i^\pi \rightarrow J_f^\pi$	$E_\gamma$ [keV]	$q^2(E0/E2)$		$\rho^2(E0) \cdot 10^3$	
		Present	Previous	Present	Previous
$0_2^+ \rightarrow 0_1^+$	854	0.210(14)	0.202(14)	25(3)	22.9(25)
$0_3^+ \rightarrow 0_2^+$	804	< 15			
$2_2^+ \rightarrow 2_1^+$	634	0.39(22)		210(130)	

634.75 keV, respectively). For this reason, the  $\alpha_K$  value could not be calculated directly and was deduced by using the expression

$$\alpha_K(2_2^+ \rightarrow 2_1^+) = \frac{N_K^{tot} - N_K(2_1^+ \rightarrow 0_1^+)}{N_\gamma(2_2^+ \rightarrow 2_1^+)} \cdot \frac{\epsilon_\gamma(2_2^+ \rightarrow 2_1^+)}{\epsilon_K} \quad (1)$$

where (i)  $\epsilon_\gamma$  and  $\epsilon_K$  are the  $\gamma$ -ray and electron efficiencies, respectively, (ii)  $N_K^{tot}$  is the total number of counts of the electron peak, (iii)  $N_\gamma(2_2^+ \rightarrow 2_1^+)$  is the number of counts for the  $2_2^+ \rightarrow 2_1^+$  transition, calculated from the number of counts measured for the  $2_2^+ \rightarrow 0_1^+$   $\gamma$  transition and their relative intensity, taken from Ref. [27], (iv)  $N_K(2_1^+ \rightarrow 0_1^+)$  is the number of counts expected for the electron  $2_1^+ \rightarrow 0_1^+$  line calculated as

$$N_K(2_1^+ \rightarrow 0_1^+) = \alpha_K^{th}(2_1^+ \rightarrow 0_1^+) N_\gamma(2_1^+ \rightarrow 0_1^+) \quad (2)$$

where  $\alpha_K^{th}(2_1^+ \rightarrow 0_1^+)$  is taken from BRICC [29] and  $N_\gamma(2_1^+ \rightarrow 0_1^+)$  is the expected number of counts for the  $2_1^+ \rightarrow 0_1^+$   $\gamma$  line. This latter value was calculated by taking into account the relative intensity [27] of the  $2_1^+ \rightarrow 0_1^+$  transition to the  $(1, 2^+) \rightarrow 0_3^+$  (at 2130 keV) and  $4_1^+ \rightarrow 2_1^+$  (at 728 keV) ones, visible in the  $\gamma$ -ray spectrum. Since the first is populated only in the  $\beta$ -decay of the ground state of  $^{74}\text{Br}$  and the other in the decay of the isomeric  $J^\pi = 4^{(+)}$  level, the two contributions have been added to obtain the total yield of the  $2_1^+ \rightarrow 0_1^+$  transition. The  $\alpha_K(2_2^+ \rightarrow 2_1^+)$  value has been evaluated using Eqs. (1), (2). The extracted  $\alpha_K(2_2^+ \rightarrow 2_1^+)$  value, large with respect to the calculated one even for a pure  $E2$  transition (see Table 1), suggests the presence of a strong  $E0$  component in this transition. From Table 1, all the other measured values are in agreement with the calculations for the expected multipolarities. For the state at 2563 keV, tentatively assigned as  $(2^+, 3, 4^+)$  in Ref. [27], we firmly establish the positive parity.

The key quantities  $q^2(E0/E2; 2_2^+ \rightarrow 2_1^+)$ , which represents the ratio between the experimental  $E0$  yield for the indicated electron transition and the  $E2$  yield for the electron transition from the initial state to the first excited  $2^+$  state [31], obtained in this work are reported in Table 2. The ratio  $q^2(E0/E2; 2_2^+ \rightarrow 2_1^+)$  and the monopole strength  $\rho^2(E0; 2_2^+ \rightarrow 2_1^+)$  were calculated from the measured  $\alpha_K(2_2^+ \rightarrow 2_1^+)$  value, together with the already known lifetime  $\tau(2_2^+)$  ps [27], the  $2_2^+ \rightarrow 2_1^+$  to  $2_2^+ \rightarrow 0_1^+$   $\gamma$  branching ratio [27], and the weighted average of the two  $\delta(E2/M1)$  values reported by Coban *et al.* ( $\delta = -5.6(16)$ ) [32] and by Cambiaggio *et al.* ( $\delta = -2.6(2)$ ) [33]. A large value  $\rho^2(E0; 2_2^+ \rightarrow 2_1^+) \cdot 10^3 = 210(130)$ , compatible with those reported in Ref. [7,8] for the Ni isotopes, is obtained for  $^{74}\text{Se}$ . This result is not in agreement with a simple vibrational picture for this nucleus with the  $2_2^+$  state as member of the two-phonon multiplet, and not even with the interpretation of the state as the head of a  $\gamma$ -band in an axially-symmetric deformed nucleus. It is also worth noticing how the weak  $B(E2; 2_2^+ \rightarrow 0_2^+) = 3.5(11)$  W.u. value [13] seems to exclude the  $2_2^+$  state as part of a shape-coexisting band built on the  $0_2^+$  state. The  $0_3^+ \rightarrow 0_2^+$  transition was not visible in our electron spectra, thus, an upper limit for the intensity of this transition was extracted as  $q^2(E0/E2) < 15$  (99.7% confidence level). From this

result, it is possible to deduce a limit for the  $\rho^2(E0; 0_3^+ \rightarrow 0_2^+)$  value assuming a  $B(E2; 0_3^+ \rightarrow 2_1^+)$  value, using the expression

$$\rho^2(E0; 0_3^+ \rightarrow 0_2^+) \cdot 10^3 = 3.28 \cdot 10^{-3} q^2(E0/E2) \cdot B(E2; 0_3^+ \rightarrow 2_1^+) \quad (3)$$

where  $3.28 \cdot 10^{-3}$  refers to known properties of the nucleus and the transitions of interest (see Ref. [31]) and the  $B(E2)$  value is in Weisskopf units. Even by assuming an unrealistically large value  $B(E2; 0_3^+ \rightarrow 2_1^+) = 100$  W.u., the corresponding  $\rho^2(E0; 0_3^+ \rightarrow 0_2^+)$  would be less than 5. This result disagrees with the hypothesis suggested in Ref. [13] of a spherical  $0_2^+$  state strongly mixed with a well-deformed, prolate  $0_3^+$  state.

#### 4. Theoretical analysis

The low-lying states in  $^{74}\text{Se}$  were further investigated with BMF calculations using the Symmetry Conserving Configuration Mixing (SCCM) framework [34] with the Gogny D1S [35] as the underlying nuclear interaction. Within this method, the intrinsic states are described as Hartree-Fock-Bogoliubov (HFB) -like wave functions obtained self-consistently through Particle-Number Variation After Projection (PN-VAP) [36]. The level energies obtained from these calculations are shown in Fig. 2 together with the experimental ones. The predicted energies agree well with the experimental values. A set of reduced  $E2$  electromagnetic matrix elements was extracted within the BMF framework. The resulting  $B(E2)$  values normalized to that of the  $2_1^+ \rightarrow 0_1^+$  transition are compared to the experimental ones in Table 3. The general agreement is good. In the same table, the  $B(E2)$  ratios are also compared to those calculated for the harmonic spherical-vibrator limit and with recently published calculations by Nomura *et al.* [37]. These authors used a theoretical framework based on the nuclear density functional theory and the interacting boson model to describe shape coexistence and quadrupole and octupole collective excitations in some transitional nuclei, including  $^{74}\text{Se}$ . The comparison shows how both our BMF and the Nomura *et al.* calculations succeed in reproducing the relative  $B(E2)$  values for the  $4_1^+ \rightarrow 2_1^+$ , and  $6_1^+ \rightarrow 4_1^+$  transitions. As for the levels of interest for the present work, the decay from the  $2_2^+$  level is better reproduced by the BMF calculations while the  $B(E2; 0_2^+ \rightarrow 2_1^+)$  value is better reproduced by the Nomura *et al.* calculations. Table 3 also reports the comparison between the experimental and calculated  $\rho^2(E0)$  values for the different models. We note that Nomura *et al.* adjusted the  $E0$  boson charge to reproduce the  $\rho^2(E0; 0_2^+ \rightarrow 0_1^+)$  value. The BMF calculations seem to overestimate the configuration mixing between the two  $0^+$  states, as indicated by the high value obtained for this quantity. As for the large  $\rho^2(E0; 2_2^+ \rightarrow 2_1^+)$  value, it is not reproduced by the calculations. In both cases, the prediction is around one fifth that of the corresponding  $\rho^2(E0; 0_2^+ \rightarrow 0_1^+)$  value whereas experimentally the  $\rho^2(E0; 2_2^+ \rightarrow 2_1^+)$  value is 5 times larger than the  $\rho^2(E0; 0_2^+ \rightarrow 0_1^+)$  one.

The  $^{74}\text{Se}$  PN-VAP energy calculated with the BMF approach in the  $(\beta_2, \gamma)$  plane is shown in Fig. 3. Three minima are visible: oblate (0.25, 60°), triaxial (0.40, 20°), and spherical, all below 2-MeV excitation energy. This result indicates the possible presence of shape coexistence. Once the shape mixing is included in the calculations, it becomes possible to describe the state's intrinsic shape through Collective Wave Functions (CWF) obtained within the SCCM framework, which represent the weights of  $(\beta_2, \gamma)$  deformation for each considered state (Fig. 4). Considering the CWFs of the different states, the level scheme has been organized into bands. Four distinctive structures are predicted: (i) the ground-state band built on top of the triaxial minimum, characterized by mixing with an oblate configuration in the ground state, which disappears at larger angular momentum, (ii) a band built on top of

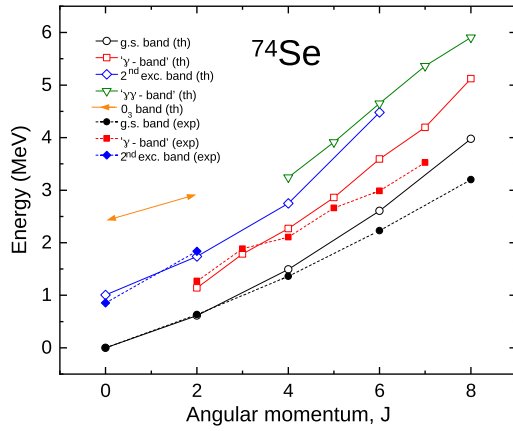


**Fig. 2.** Comparison between experimental level energies in  $^{74}\text{Se}$  and corresponding BMF calculations. The labelling follows the band structure suggested in the present paper (see Fig. 4). A  $\gamma\gamma$  band and a band built on the  $0_3^+$  state are also suggested by the calculations (green and orange, respectively).

**Table 3**

Comparison of experimental relative  $B(E2)$  and  $\rho^2(E0)$  values with different theoretical calculations. The experimental data are taken from the present work and from Ref. [13]. The calculated values are from the harmonic spherical vibrational limit, the present BMF calculations, and the Nomura *et al.* calculations [37]. The relative  $B(E2)$  values are normalized to the  $B(E2; 2_1^+ \rightarrow 0_1^+)$  values, which are reported in Weisskopf units in the first row.

Observable	Exp.	Vibr.	BMF	Nomura <i>et al.</i>
$B(E2; 2_1^+ \rightarrow 0_1^+)$ [W.u.]	42.0(6)		68	42
$B_{\text{rel}}(E2; 4_1^+ \rightarrow 2_1^+)$	1.90(2)	2	1.69	1.88
$B_{\text{rel}}(E2; 0_2^+ \rightarrow 2_1^+)$	1.83(2)	2	0.94	1.50
$B_{\text{rel}}(E2; 2_2^+ \rightarrow 2_1^+)$	1.12(10)	2	1.47	0.16
$B_{\text{rel}}(E2; 2_2^+ \rightarrow 0_2^+)$	0.08(11)	0	0.19	0.52
$B_{\text{rel}}(E2; 6_1^+ \rightarrow 4_1^+)$	1.71(6)	3	2.27	2.14
$\rho^2(E0; 0_2^+ \rightarrow 0_1^+) \cdot 10^3$	25(3)	0	154	23
$\rho^2(E0; 2_2^+ \rightarrow 2_1^+) \cdot 10^3$	210(130)	0	26	4.9

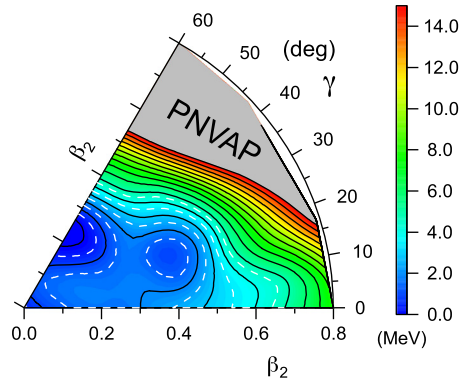


**Fig. 3.** Potential energy surface for  $^{74}\text{Se}$  resulting from deformation-constrained Hartree-Fock calculations with the particle number projection method (PN-VAP) and the Gogny D1S interaction.

the triaxial  $2_2^+$  state, associated with the ground-state band, (iii) the band built on the  $0_2^+$  state with strong mixing of the oblate and triaxial configurations, (iv) the band built on the  $0_3^+$  state with strong mixing of the prolate and triaxial configurations. Because of the emerging triaxiality in the calculations, the band (ii) does not follow the requirements of a  $\gamma$  band as defined for an axially-symmetric rotor. Indeed, the calculated wavefunction of the  $2_2^+$  state is 49%  $K=0$  and 51%  $|K|=2$ . In the band built on the  $0_2^+$  state, the degree of mixing changes with angular momentum, with the  $0^+$ ,  $2^+$ ,  $4^+$  states more oblate than triaxial, and the  $6^+$  state more triaxial than oblate. A remarkable aspect of the BMF

calculations is that they do not support a spherical vibrational interpretation for the low-lying states of  $^{74}\text{Se}$ . All the states show significant deformation and none of them have vibrational wave functions.

Concerning the  $\rho^2(E0)$  values, it is visible from Fig. 4 that the configurations of the  $0_2^+$  and  $0_3^+$  states are different, supporting the interpretation of small mixing and resulting in a small  $\rho^2(E0; 0_3^+ \rightarrow 0_2^+)$  value. For the  $\rho^2(E0; 2_2^+ \rightarrow 2_1^+)$  value, it is interesting how our BMF calculations allow for a quite strong  $E0$  transition. This is due to the triaxiality of the  $2_2^+$  and  $2_1^+$  states and their mixed  $K$  values.

## 5. Conclusion

A set of internal K-conversion coefficients and electric monopole transition strengths in the  $^{74}\text{Se}$  isotope has been deduced. The obtained  $\rho^2(E0; 2_2^+ \rightarrow 2_1^+)$  value points out another enhanced electric monopole transition between the  $2_1^+$  and  $2_2^+$  states, similar to those recently observed in the close Ni isotopes. Also, the upper limit deduced for the electron intensity of the  $0_3^+ \rightarrow 0_2^+$  transition is not in agreement with the previous explanation of the low energy of the  $0_2^+$  state given in Ref. [13], *i.e.*, a spherical state strongly mixed with a well-deformed, prolate  $0_3^+$  state. Our BMF calculations generally reproduce the experimental quantities, except for the  $\rho^2(E0)$  values. In particular, the  $\rho^2(E0; 2_2^+ \rightarrow 2_1^+)$  value is underestimated by a factor of  $\approx 7$ . The present SCCM can be extended by including additional collective and single-particle degrees of freedom that could produce a larger overlap between the states. However, this is still highly demanding from the computational point of view. Interestingly, though, the calculated  $\rho^2(E0; 2_2^+ \rightarrow 2_1^+)$  value is large, contrary to what is expected for a simpler structure of  $^{74}\text{Se}$ . The  $0_2^+$  state is interpreted as a shape coexisting state in the calculations, and the  $2_2^+$  state is the head of another band at low excitation energy. However, the structure of this latter band does not follow the requirements of a pure  $\gamma$  band. A more complex shape coexistence and mixing scenario is pictured for  $^{74}\text{Se}$  at low-excitation energy. Noteworthy, both the experimental results and the theoretical calculations agree with removing another isotope from the list of candidate vibrators. Instead, triaxiality and multiple-shape coexistence are suggested, two phenomena traditionally thought to be rare that recently seem to appear in more and more mid-mass nuclei. Further measurements of  $B(E2)$  and  $\rho^2(E0)$  values, and ultimately the determination of quadrupole invariants via low-energy Coulomb excitation, are envisaged for this mass region.

## Declaration of competing interest

The authors declare that they have no known competing financial interests or personal relationships that could have appeared to influence the work reported in this paper.

## Data availability

Data will be made available on request.

## Acknowledgements

The authors thank the staff of the LNL Tandem-XTU accelerator for the high quality of the delivered  $^{16}\text{O}$  beam, M. Loriggiola for producing the targets, and the mechanical workshops of the INFN division of Florence for their contribution.

T.R. Rodríguez acknowledges funding from the Spanish MICIN under contract PID2021-127890NB-I00 and support from GSI-Darmstadt computing facility.

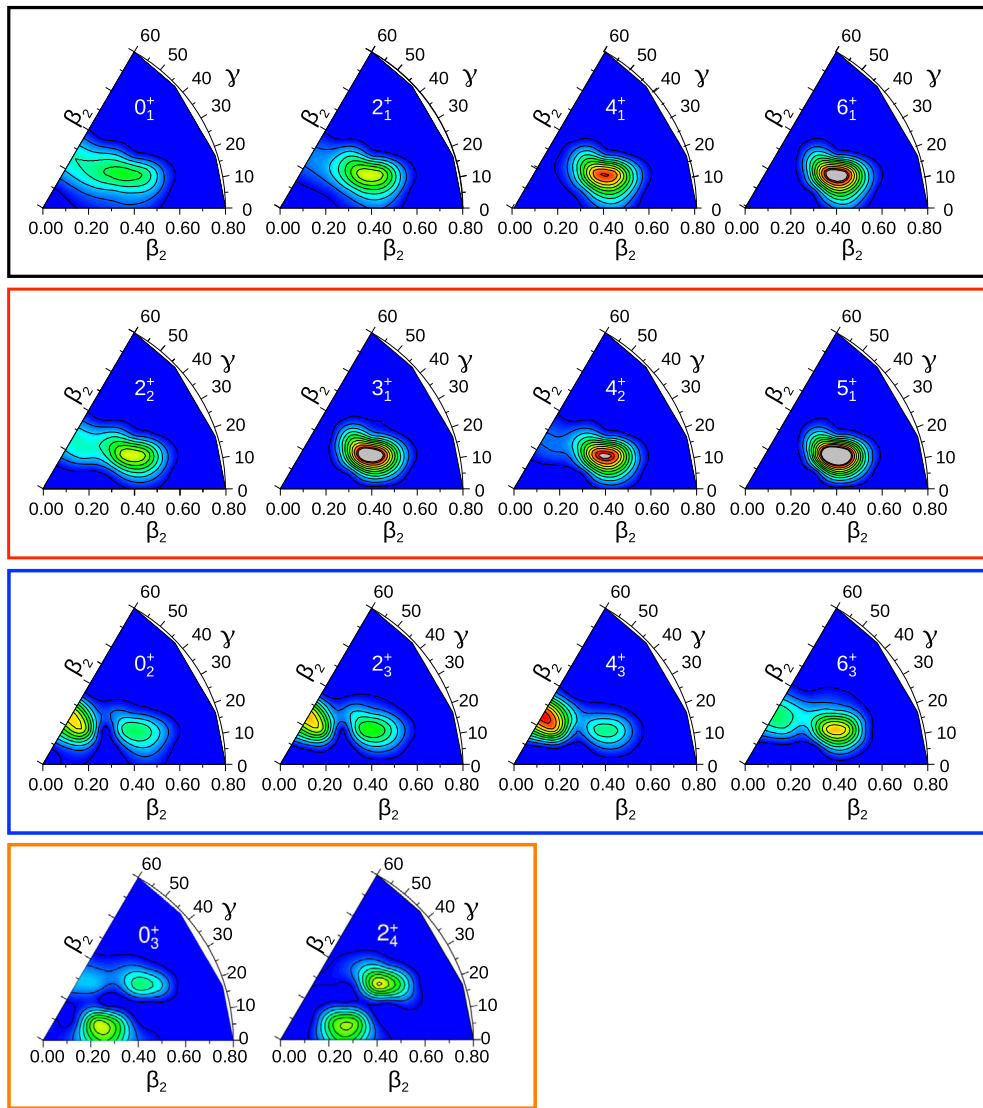


**Fig. 4.** Collective wave functions (CWT) calculated for low-lying states in  $^{74}\text{Se}$ . The  $\gamma$  deformation parameter is given in degrees. The states are organized in bands: the ground state band (black), the band based on the  $2_2^+$  state (red), a band built on the  $0_2^+$  state (blue), and a band built on the  $0_3^+$  state (orange).

## References

- [1] P.E. Garrett, J.L. Wood, On the robustness of surface vibrational modes: case studies in the Cd region, *J. Phys. G, Nucl. Part. Phys.* 37 (6) (2010) 064028, <https://doi.org/10.1088/0954-3899/37/6/064028>.
- [2] P.E. Garrett, T.R. Rodríguez, A.D. Varela, K.L. Green, J. Bangay, A. Finlay, R.A.E. Austin, G.C. Ball, D.S. Bandyopadhyay, V. Bildstein, S. Colosimo, D.S. Cross, G.A. Demand, P. Finlay, A.B. Garnsworthy, G.F. Grinyer, G. Hackman, B. Jigmeddorj, J. Jolie, W.D. Kulp, K.G. Leach, A.C. Morton, J.N. Orce, C.J. Pearson, A.A. Phillips, A.J. Radich, E.T. Rand, M.A. Schumaker, C.E. Svensson, C. Sumithrarachchi, S. Triambak, N. Warr, J. Wong, J.L. Wood, S.W. Yates, Multiple shape coexistence in  $^{110,112}\text{Cd}$ , *Phys. Rev. Lett.* 123 (2019) 142502, <https://doi.org/10.1103/PhysRevLett.123.142502>.
- [3] P.E. Garrett, T.R. Rodríguez, A. Diaz Varela, K.L. Green, J. Bangay, A. Finlay, R.A.E. Austin, G.C. Ball, D.S. Bandyopadhyay, V. Bildstein, S. Colosimo, D.S. Cross, G.A. Demand, P. Finlay, A.B. Garnsworthy, G.F. Grinyer, G. Hackman, B. Jigmeddorj, J. Jolie, W.D. Kulp, K.G. Leach, A.C. Morton, J.N. Orce, C.J. Pearson, A.A. Phillips, A.J. Radich, E.T. Rand, M.A. Schumaker, C.E. Svensson, C. Sumithrarachchi, S. Triambak, N. Warr, J. Wong, J.L. Wood, S.W. Yates, Shape coexistence and multiparticle-multihole structures in  $^{110,112}\text{Cd}$ , *Phys. Rev. C* 101 (2020) 044302, <https://doi.org/10.1103/PhysRevC.101.044302>.
- [4] P.E. Garrett, Characterization of the  $\beta$  vibration and  $0_2^+$  states in deformed nuclei, *J. Phys. G, Nucl. Part. Phys.* 27 (1) (2001) R1, <https://doi.org/10.1088/0954-3899/27/1/201>.
- [5] K. Heyde, J.L. Wood, Shape coexistence in atomic nuclei, *Rev. Mod. Phys.* 83 (2011) 1467–1521, <https://doi.org/10.1103/RevModPhys.83.1467>.
- [6] J.L. Wood, E.F. Zganjar, C. De Coster, K. Heyde, Electric monopole transitions from low energy excitations in nuclei, *Nucl. Phys. A* 651 (4) (1999) 323–368, [https://doi.org/10.1016/S0375-9474\(99\)00143-8](https://doi.org/10.1016/S0375-9474(99)00143-8).
- [7] L.J. Evitts, A.B. Garnsworthy, T. Kibédi, J. Smallcombe, M.W. Reed, B.A. Brown, A.E. Stuchbery, G.J. Lane, T.K. Eriksen, A. Akber, B. Alshahrani, M. de Vries, M.S.M. Gerathy, J.D. Holt, B.Q. Lee, B.P. McCormick, A.J. Mitchell, M. Moukaddam, S. Mukhopadhyay, N. Palalani, T. Palazzo, E.E. Peters, A.P.D. Ramirez, S.R. Stroberg, T. Tornyi, S.W. Yates, Identification of significant E0 strength in the  $2_2^+ \rightarrow 2_1^+$  transitions of  $^{58,60,62}\text{Ni}$ , *Phys. Lett. B* 779 (2018) 396–401, <https://doi.org/10.1016/j.physletb.2018.01.076>.
- [8] L.J. Evitts, A.B. Garnsworthy, T. Kibédi, J. Smallcombe, M.W. Reed, A.E. Stuchbery, G.J. Lane, T.K. Eriksen, A. Akber, B. Alshahrani, M. de Vries, M.S.M. Gerathy, J.D. Holt, B.Q. Lee, B.P. McCormick, A.J. Mitchell, M. Moukaddam, S. Mukhopadhyay, N. Palalani, T. Palazzo, E.E. Peters, A.P.D. Ramirez, T. Tornyi, S.W. Yates, E0 transition strength in stable Ni isotopes, *Phys. Rev. C* 99 (2019) 024306, <https://doi.org/10.1103/PhysRevC.99.024306>.
- [9] T. Kibédi, A. Garnsworthy, J. Wood, Electric monopole transitions in nuclei, *Prog. Part. Nucl. Phys.* 123 (2022) 103930, <https://doi.org/10.1016/j.pnpnp.2021.103930>.
- [10] E.B. Shera, E.T. Ritter, R.B. Perkins, G.A. Rinker, L.K. Wagner, H.D. Wohlfahrt, G. Fricke, R.M. Steffen, Systematics of nuclear charge distributions in Fe, Co, Ni, Cu, and Zn deduced from muonic x-ray measurements, *Phys. Rev. C* 14 (1976) 731–747, <https://doi.org/10.1103/PhysRevC.14.731>.
- [11] A. Steudel, U. Triebe, D. Wendlandt, Isotope shift in Ni I and changes in mean-square nuclear charge radii of the stable Ni isotopes, *Z. Phys. A* 296 (3) (1980) 189–193, <https://doi.org/10.1007/BF01415832>.

- [12] P. Raghavan, Table of nuclear moments, *At. Data Nucl. Data Tables* 42 (2) (1989) 189–291, [https://doi.org/10.1016/0092-640X\(89\)90008-9](https://doi.org/10.1016/0092-640X(89)90008-9).
- [13] E.A. McCutchan, C.J. Lister, T. Ahn, V. Anagnostatou, N. Cooper, M. Elvers, P. Goddard, A. Heinz, G. Ilie, D. Radeck, D. Savran, V. Werner, Shape coexistence and high-K states in  $^{74}\text{Se}$  populated following the  $\beta$  decay of  $^{74}\text{Br}$ , *Phys. Rev. C* 87 (2013) 014307, <https://doi.org/10.1103/PhysRevC.87.014307>.
- [14] P.D. Cottle, J.W. Holcomb, T.D. Johnson, K.A. Stuckey, S.L. Tabor, P.C. Womble, S.G. Buccino, F.E. Durham, Shape coexistence and octupole vibrations in  $^{74}\text{Se}$ , *Phys. Rev. C* 42 (1990) 1254–1263, <https://doi.org/10.1103/PhysRevC.42.1254>.
- [15] J. Döring, G.D. Johns, M.A. Riley, S.L. Tabor, Y. Sun, J.A. Sheikh, Band structures and alignment properties in  $^{74}\text{Se}$ , *Phys. Rev. C* 57 (1998) 2912–2923, <https://doi.org/10.1103/PhysRevC.57.2912>.
- [16] J. Ljungvall, A. Görge, M. Girod, J.P. Delaroche, A. Dewald, C. Dossat, E. Farnea, W. Kortzen, B. Melon, R. Menegazzo, A. Obertelli, R. Orlandi, P. Petkov, T. Pissulla, S. Siem, R.P. Singh, J. Srebrny, C. Theisen, C.A. Ur, J.J. Valiente-Dobón, K.O. Zell, M. Zielińska, Shape coexistence in Light Se isotopes: evidence for oblate shapes, *Phys. Rev. Lett.* 100 (2008) 102502, <https://doi.org/10.1103/PhysRevLett.100.102502>.
- [17] J. Henderson, C.Y. Wu, J. Ash, P.C. Bender, B. Elman, A. Gade, M. Grinder, H. Iwasaki, E. Kwan, B. Longfellow, T. Mijatović, D. Rhodes, M. Spieker, D. Weisshaar, Localizing the shape transition in neutron-deficient Selenium, *Phys. Rev. Lett.* 121 (2018) 082502, <https://doi.org/10.1103/PhysRevLett.121.082502>.
- [18] N. Hinohara, K. Sato, T. Nakatsukasa, M. Matsuo, K. Matsuyanagi, Microscopic description of large-amplitude shape-mixing dynamics with inertial functions derived in local quasiparticle random-phase approximation, *Phys. Rev. C* 82 (2010) 064313, <https://doi.org/10.1103/PhysRevC.82.064313>.
- [19] J. Smallcombe, A.B. Garnsworthy, W. Kortzen, P. Singh, F.A. Ali, C. Andreoiu, S. Ansari, G.C. Ball, C.J. Barton, S.S. Bhattacharjee, M. Bowry, R. Caballero-Folch, A. Chester, S.A. Gillespie, G.F. Grinyer, G. Hackman, C. Jones, B. Melon, M. Moukadam, A. Nannini, P. Ruotsalainen, K. Starosta, C.E. Svensson, R. Wadsworth, J. Williams, Improved measurement of the  $0_2^+ \rightarrow 0_1^+$  E0 transition strength for  $^{72}\text{Se}$  using the spice spectrometer, *Phys. Rev. C* 106 (2022) 014312, <https://doi.org/10.1103/PhysRevC.106.014312>.
- [20] J. Henderson, C.Y. Wu, J. Ash, B.A. Brown, P.C. Bender, R. Elder, B. Elman, A. Gade, M. Grinder, H. Iwasaki, B. Longfellow, T. Mijatović, D. Rhodes, M. Spieker, D. Weisshaar, Triaxiality in selenium-76, *Phys. Rev. C* 99 (2019) 054313, <https://doi.org/10.1103/PhysRevC.99.054313>.
- [21] S. Leoni, B. Fornal, N. Mărginean, M. Sferrazza, Y. Tsunoda, T. Otsuka, G. Bocchi, F.C.L. Crespi, A. Bracco, S. Aydin, M. Boromiza, D. Bucurescu, N. Cieplicka-Oryńczak, C. Costache, S. Călinescu, N. Florea, D.G. Ghiță, T. Glodariu, A. Ionescu, L. Iskra, M. Krzysiek, R. Mărginean, C. Mihai, R.E. Mihai, A. Mitu, A. Negreț, C.R. Niță, A. Olăcel, A. Oprea, S. Pascu, P. Petkov, C. Petrone, G. Porzio, A. Șerban, C. Sotty, L. Stan, I. Știru, L. Stroe, R. Șuvăilă, S. Toma, A. Turturică, S. Ujenuic, C.A. Ur, Multifaceted quadruplet of low-lying spin-zero states in  $^{66}\text{Ni}$ : emergence of shape isomerism in light nuclei, *Phys. Rev. Lett.* 118 (2017) 162502, <https://doi.org/10.1103/PhysRevLett.118.162502>.
- [22] N. Mărginean, D. Little, Y. Tsunoda, S. Leoni, R.V.F. Janssens, B. Fornal, T. Otsuka, C. Michelagnoli, L. Stan, F.C.L. Crespi, C. Costache, R. Lica, M. Sferrazza, A. Turturică, A.D. Ayangeakaa, K. Auranen, M. Barani, P.C. Bender, S. Bottoni, M. Boromiza, A. Bracco, S. Călinescu, C.M. Campbell, M.P. Carpenter, P. Chowdhury, M. Ciemala, N. Cieplicka-Oryńczak, D. Cline, C. Clisu, H.L. Crawford, I.E. Dinescu, J. Dudouet, D. Filipescu, N. Florea, A.M. Forney, S. Fracassetti, A. Gade, I. Gheorghe, A.B. Hayes, I. Harca, J. Henderson, A. Ionescu, L.W. Iskra, M. Jentschel, F. Kandzia, Y.H. Kim, F.G. Kondev, G. Korschinek, U. Köster, Krishichayan, M. Krzysiek, T. Lauritsen, J. Li, R. Mărginean, E.A. Mauger, C. Mihai, R.E. Mihai, A. Mitu, P. Mutti, A. Negreț, C.R. Niță, A. Olăcel, A. Oprea, S. Pascu, C. Petrone, C. Porzio, D. Rhodes, D. Seweryniak, D. Schumann, C. Sotty, S.M. Stolze, R. Șuvăilă, S. Toma, S. Ujenuic, W.B. Walters, C.Y. Wu, J. Wu, S. Zhu, S. Ziliani, Shape coexistence at zero spin in  $^{64}\text{Ni}$  driven by the monopole tensor interaction, *Phys. Rev. Lett.* 125 (2020) 102502, <https://doi.org/10.1103/PhysRevLett.125.102502>.
- [23] A.D. Ayangeakaa, R.V.F. Janssens, C.Y. Wu, J.M. Allmond, J.L. Wood, S. Zhu, M. Albers, S. Almaraz-Calderon, B. Bucher, M.P. Carpenter, C.J. Chiara, D. Cline, H.L. Crawford, H.M. David, J. Harker, A.B. Hayes, C.R. Hoffman, B.P. Kay, K. Kolos, A. Korichi, T. Lauritsen, A.O. Macchiavelli, A. Richard, D. Seweryniak, A. Wiens, Shape coexistence and the role of axial asymmetry in  $^{72}\text{Ge}$ , *Phys. Lett. B* 754 (2016) 254–259, <https://doi.org/10.1016/j.physletb.2016.01.036>.
- [24] A.D. Ayangeakaa, R.V.F. Janssens, S. Zhu, D. Little, J. Henderson, C.Y. Wu, D.J. Hartley, M. Albers, K. Auranen, B. Bucher, M.P. Carpenter, P. Chowdhury, D. Cline, H.L. Crawford, P. Fallon, A.M. Forney, A. Gade, A.B. Hayes, F.G. Kondev, Krishichayan, T. Lauritsen, J. Li, A.O. Macchiavelli, D. Rhodes, D. Seweryniak, S.M. Stolze, W.B. Walters, J. Wu, Evidence for rigid triaxial deformation in  $^{76}\text{Ge}$  from a model-independent analysis, *Phys. Rev. Lett.* 123 (2019) 102501, <https://doi.org/10.1103/PhysRevLett.123.102501>.
- [25] M. Rocchini, K. Hadyńska-Klęk, A. Nannini, A. Goasduff, M. Zielińska, D. Testov, T.R. Rodríguez, A. Gargano, F. Nowacki, G. De Gregorio, H. Naïdja, P. Sona, J.J. Valiente-Dobón, D. Mengoni, P.R. John, D. Bazzacco, G. Benzoni, A. Boso, P. Cocconi, M. Chiari, D.T. Doherty, F. Galtarossa, G. Jaworski, M. Komorowski, N. Marchini, M. Matejska-Minda, B. Melon, R. Menegazzo, P.J. Napiorkowski, D. Napoli, M. Ottanelli, A. Perego, L. Ramina, M. Rampazzo, F. Recchia, S. Riccetto, D. Rosso, M. Siciliano, Onset of triaxial deformation in  $^{66}\text{Zn}$  and properties of its first excited  $0^+$  state studied by means of coulomb excitation, *Phys. Rev. C* 103 (2021) 014311, <https://doi.org/10.1103/PhysRevC.103.014311>.
- [26] M. Rocchini, P.E. Garrett, M. Zielińska, S.M. Lenzi, D.D. Dao, F. Nowacki, V. Bildstein, A.D. MacLean, B. Olaizola, Z.T. Ahmed, C. Andreoiu, A. Babu, G.C. Ball, S.S. Bhattacharjee, H. Bidaman, C. Cheng, R. Coleman, I. Dillmann, A.B. Garnsworthy, S. Gillespie, C.J. Griffin, G.F. Grinyer, G. Hackman, M. Hanley, A. Illana, S. Jones, A.T. Laffoley, K.G. Leach, R.S. Lubna, J. McAfee, C. Natzke, S. Pannu, C. Paxman, C. Porzio, A.J. Radich, M.M. Rajabali, F. Sarazin, K. Schwarz, S. Shadrack, S. Sharma, J. Suh, C.E. Svensson, D. Yates, T. Zidar, First evidence of axial shape asymmetry and configuration coexistence in  $^{74}\text{Zn}$ : suggestion for a northern extension of the  $N=40$  island of inversion, *Phys. Rev. Lett.* 130 (2023) 122502, <https://doi.org/10.1103/PhysRevLett.130.122502>.
- [27] B. Singh, A.R. Farhan, Nuclear Data Sheets for  $A=74$ , *Nucl. Data Sheets* 107 (2006) 1923–2102, <https://doi.org/10.1016/j.nds.2006.05.006>.
- [28] T. Fazzini, A. Giannatiempo, A. Perego, A magnetic transport electron spectrometer for in-beam measurements, *Nucl. Instrum. Methods Phys. Res.* 211 (1) (1983) 125–128, [https://doi.org/10.1016/0167-5087\(83\)90560-4](https://doi.org/10.1016/0167-5087(83)90560-4).
- [29] Research school of physics anu college of science bric conversion coefficient calculator, <https://bricc.anu.edu.au/> (Updated: 12 April 2023).
- [30] H.C. Pauli, K. Alder, R.M. Steffen, *The Electromagnetic Interaction in Nuclear Spectroscopy*, W.D. Hamilton, 1975.
- [31] T. Kibédi, R.H. Spear, Electric monopole transitions between  $0^+$  states for nuclei throughout the periodic table, *At. Data Nucl. Data Tables* 89 (1) (2005) 77–100, <https://doi.org/10.1016/j.adt.2004.11.002>.
- [32] A. Coban, J.C. Lisle, G. Murray, J.C. Willmott, States of  $^{74}\text{Se}$  observed following decay of  $^{74}\text{Br}$ , *Part. Nucl.* 4 (1972).
- [33] M.C. Cambiaggio, G. Garcia Bermúdez, M. Behar, The spin of the 2.198 keV level in  $^{74}\text{Ge}$  and multipole mixing ratios of gamma transitions in the decay of  $^{74}\text{As}$ , *Z. Phys. A* 275 (1975), <https://doi.org/10.1007/BF01409595>.
- [34] T.R. Rodríguez, J.L. Egido, Triaxial angular momentum projection and configuration mixing calculations with the Gogny force, *Phys. Rev. C* 81 (2010) 064323, <https://doi.org/10.1103/PhysRevC.81.064323>.
- [35] J.F. Berger, M. Girod, D. Gogny, Microscopic analysis of collective dynamics in low energy fission, *Nucl. Phys. A* 428 (1984) 23–36, [https://doi.org/10.1016/0375-9474\(84\)90240-9](https://doi.org/10.1016/0375-9474(84)90240-9).
- [36] M. Anguiano, J.L. Egido, L.M. Robledo, Particle number projection with effective forces, *Nucl. Phys. A* 696 (3) (2001) 467–493, [https://doi.org/10.1016/S0375-9474\(01\)01219-2](https://doi.org/10.1016/S0375-9474(01)01219-2).
- [37] K. Nomura, Effect of configuration mixing on quadrupole and octupole collective states of transitional nuclei, *Phys. Rev. C* 106 (2022) 024330, <https://doi.org/10.1103/PhysRevC.106.024330>.